http://dx.doi.org/10.5935/0103-5053.20140064

J. Braz. Chem. Soc., Vol. 25, No. 5, 928-934, 2014.
Printed in Brazil - ©2014 Sociedade Brasileira de Química
0103 - 5053 $6.00+0.00

Article

SPR Biosensors Based on Gold and Silver Nanoparticle Multilayer Films

Antônio L. C. M. da Silva,[a] Marony G. Gutierres,[a] Anderson Thesing,[a] Rafael M. Lattuada[¥,b] and Jacqueline Ferreira[,#,a]*

[a]*Centro de Ciências Químicas, Farmacêuticas e de Alimentos, Universidade Federal de Pelotas, CP 354, 96010-900 Pelotas-RS, Brazil*

[b]*Instituto de Química, Universidade Federal do Rio Grande do Sul, CP 15003, 91501-970 Porto Alegre-RS, Brazil*

Filmes em multicamadas de nanopartículas de ouro e prata foram utilizados para o desenvolvimento de um sensor plasmônico para detecção de ligações entre moléculas orgânicas e/ou com atividade biológicas. A sensibilidade a eventos de ligação é relacionada a deslocamentos energéticos da ressonância de plasmon de superfície nos filmes de nanopartículas metálicas. Quando aplicado como sensor de *bulk* (sensibilidade às mudanças no índice de refração do meio em contato com a superfície do metal), a sensibilidade foi ca. 220 ± 33 nm RIU^{-1} para filmes de nanopartículas de ouro e 140 ± 10 nm RIU^{-1} para filmes de nanopartículas de prata. Na aplicação como sensor de superfície (sensibilidade às mudanças no índice de refração efetivo, devido às adsorções na superfície do metal) para detecção de moléculas biológicas, o sensor mostrou-se eficiente na detecção da proteína estreptavidina, através da sua interação por bioafinidade com biotina. As principais vantagens relacionadas com o biossensor plasmônico desenvolvido neste trabalho consistem na simplicidade e baixo custo da metodologia utilizada, quando comparada com outras amostras, como as fabricadas por feixe de íons focado (FIB). Adicionalmente, o biossensor desenvolvido apresentou sensibilidade semelhante à de matrizes de nanoburacos e de grades de relevo, permitindo, como nestes casos, que a detecção seja feita através de medidas em tempo real.

Gold and silver nanoparticle multilayer films were used for the development of a plasmonic sensor, applied to detect surface binding of organic and/or biological molecules. The sensitivity to binding events is related to energetic shifts of the surface plasmon resonance on the film. When applied as a bulk sensor (sensitivity to changes on refractive index of the medium in contact with the metal surface), the sensitivity was found to be ca. 220 ± 33 nm RIU^{-1} for gold and ca. 140 ± 10 nm RIU^{-1} for silver nanoparticles. The systems were also found efficient as surface biosensors (sensitivity to changes on the effective refractive index due to adsorptions on the metal surface) detecting the surface binding of biotin-streptavidin protein system. The main advantage of the plasmonic biosensor developed in this work is the use of a very simple and low cost methodology when compared to fancier approaches, such as the ones using focused ion beam and surface relief gratings, although presenting similar sensitivity, and allowing, as for these cases, real-time measurements.

Keywords: SPR, gold nanoparticles, silver nanoparticles, biosensor, protein

Introduction

In the last decade, many research groups have devoted their efforts to the study and development of biosensors presenting high sensitivity and low detection limit for monitoring biological binding events.[1,2] Within this context, different nanostructured materials based on metals, oxides and semiconductors have been extensively applied.[3-7]

Recently, surface plasmon resonance (SPR) based sensors has probably become one of the most studied approaches, presenting many advantages, including high sensitivity, selectivity, speed and reliability in analysis, besides enabling real-time measurements. In addition, SPR based biosensors is attractive for allowing portability, miniaturization and site analysis.[8]

*e-mail: jacqueline.research@gmail.com
[¥]PresentAddress: Carl Zeiss do Brasil Ltda. Microscopy Division. Av. Carlos Gomes, 1.492, 90480-002 Porto Alegre-RS, Brazil
[#]Present Address: Instituto de Química, Universidade Federal do Rio Grande do Sul, C. P. 15003, 91501-970 Porto Alegre-RS, Brazil

SPR has been widely applied for the characterization and quantification of binding events in biomedical and biochemical research due to all the advantages mentioned above. Despite the short-term research of this technology, many works are focused on the understanding and controlling of the parameters related to the sensing properties. Gold and silver nanoparticles are among the most studied nanostructured materials due to the highly stable optical and chemical properties of gold and the sharp SPR signal from silver.[9,10]

In the last decade, the literature has shown that metallic nanoparticle multilayer structure simplify optical alignment and facilitate assembling of sensors using suitable binder systems.[11-13] An important advantage of this method is the versatility arising due the capability to control parameters such as film thickness in nanometric scale. In addition, this method allows the assembling of layers with specific properties and the analysis of smaller volumes than used for colloidal solution.

The performance of the sensor is defined by a few characteristics such as speed of analysis, miniaturization, sensitivity, limit of detection and figure of merit (FOM).[14-18] Table 1 summarizes the sensitivities and FOM of some plasmonic platforms fabricated with different methods.

In earlier works, we demonstrated the utilization of the enhanced transmission as an analytical probe to monitor surface binding events at the molecular level. These probes were applied for quantifying the sensitivity of both nanohole SPR configuration and surface relief gratings to detect surface binding of organic and biological molecules.[17,20,24-27] In the present work, gold and silver multilayer films were assembled on glass slides to produce a simple SPR platform. The sensors were assembled without the need of expensive infrastructure and they operate in transmission mode, allowing for a simple arrangement and providing a small probing area.

Experimental

Synthesis of nanoparticles

Gold colloidal nanoparticles were prepared according to previous methods reported in the literature.[28,29] A 1 mmol L^{-1} $HAuCl_4.3H_2O$ aqueous solution (100 mL) was refluxed at 120 °C under vigorous stirring, in silicone bath. After 10 mmol L^{-1} $C_6H_5Na_3O_7$ (2.5 mL) was quickly added to the reaction vessel. A sudden color change from pale yellow to red indicates the synthesis of the gold nanoparticles. Ultrapure water was used throughout the experiments.

Silver nanoparticles were obtained by reducing $AgNO_3$ with $NaBH_4$ at low temperature. A 1 mmol L^{-1} $AgNO_3$ solution was added drop by drop in 6 mmol L^{-1} $NaBH_4$ solution immersed in an ice bath under vigorous stirring.[30] A color change to yellow indicates the synthesis of the silver nanoparticles. Both nanoparticle solutions were concentrated by centrifuging at 13,000 rpm during 30 minutes.

Assembling gold and silver nanoparticle multilayers

The films were assembled on 1 cm^2 area of a glass slide (3.0 × 1.0 cm^2) or on fluorine doped tin oxide (FTO) glass slides (for electrochemical measurements). The substrates were previously cleaned with a mixture of 3:1 concentrated sulfuric acid and hydrogen peroxide and then immersed in 10 mmol L^{-1} $C_6H_{16}SSiO_3$ (MPTMS, 3-mercaptopropyl trimethoxysilane) methanolic solution. The initial adsorption takes few minutes, however 24 hours pause was allowed in order to obtain high molecular organizational level. The substrates were washed with methanol to remove nonadsorbed MPTMS molecules and then immersed in concentrated gold nanoparticles solution. To obtain the second nanoparticle layer, the substrate was dipped in

Table 1. Performance of biosensors based on plasmonic materials

Fabrication technique	Plasmonic nanostructure	Sensitivity / (nm RIU^{-1})	FOM / (RIU^{-1})
FIB[19]	Square arrays of circular nanoholes in Au films	333	12
FIB[20]	Square arrays of circular nanoholes in Au/SiO_x films – "in-hole detection"	650	16
Interference lithography[17]	Square arrays of circular nanoholes in Au films	271	12
Stencil lithography[21]	Square arrays of Au nanodots	179	3.2
Electrodeposition[22]	Ag nanoparticles on ITO	123	1.5
Electrodeposition[22]	Ag@Au nanoparticles on ITO	220	2.6
Pulsed laser[23]	Ag nanoparticles array	62	0.7
Pulsed laser[23]	Ag-Co bimetallic nanoparticles arrays	105	1.3

25 mL aqueous solution containing 300 μL of MPTMS and 250 μL of HCl 0.1 mol L^{-1} and once again immersed in nanoparticle solution. This step may be repeated as many times as the desired number of layers. The number of layers was based on a preliminary study to determine the highest sensitivity that resulted in 20 layers for gold and 5 layers for silver. This procedure was previously described by Fan *et al.*, where was applied to obtain silver nanoparticle multilayers film.[31]

Electrochemical characterization of the nanoparticles/MPTMS layers

The multilayer films were characterized by cyclic voltammetry (CV) blocking experiments of 1 mmol L^{-1} $K_3[Fe(CN)_6]$ and 0.1 mol L^{-1} KCl at scan rate of 100 mV s^{-1}, using a potentiostat/galvanostat Autolab model Pgstat 30. The experiments were carried out in a three compartment electrochemical cell. The multilayer films on FTO-glass were used as working, Ag|AgCl as reference and Pt wire as counter electrode.

Optical and morphological measurements

Absorption spectra from nanoparticles in solution and from the multilayer films assembled on glass slides were acquired with a Perkin-Elmer Lambda 25 spectrophotometer. The absorbed light intensity was digitally recorded in the range from 370 to 800 nm. Images of gold and silver nanoparticles were obtained using a transmission electron microscope (TEM), Carl Zeiss Inc., model Libra 120, equipped with omega filter and operated at 120 kV.

The colloid suspension was obtained in water and further dispersed using an ultrasonic bath, for 10 minutes. The samples were deposited on copper grids with a carbon film (200 mesh, from PELCO®), which were carefully heated at 50-60 °C for evaporating the solvent.

Sensitivity measurements

Solutions with known refractive index were used to measure the sensitivity of the multilayer films of nanoparticles. Aqueous $C_6H_{12}O_6$ solutions with refractive index ranging from 1.332 (diluted glucose solution) to 1.359 (concentrated glucose solution) were employed. The refractive index of each solution was determined with a refractometer Atago. For all the measurements, we have used a flow cell made of Teflon with a 25.4 mm × 25.4 mm chamber, containing a single inlet and a single outlet. The flow cell hold the sample and the solution flows over the entire surface with purging processes between each solution. The details of the chemicals employed in the on-chip assembly of the cysteamine-biotin-streptavidin system can be found elsewhere.[19] Real-time acquisition was allowed by using a peristaltic pump. All the sensitivity measurements were carried out in triplicate with three different plasmonic substrates.

Results and Discussion

Figure 1 shows TEM images of gold and silver nanoparticles obtained in this work. One can observe the formation of nearly spherical nanoparticles for both samples (identified by energy dispersive spectroscopy - not shown). The nanoparticles diameter may be estimated as 30 nm (Figure 1a) and 11 nm (Figure 1b), for gold and silver, respectively. For the latter, large nanoparticle agglomerates and large particle size distribution were also observed.

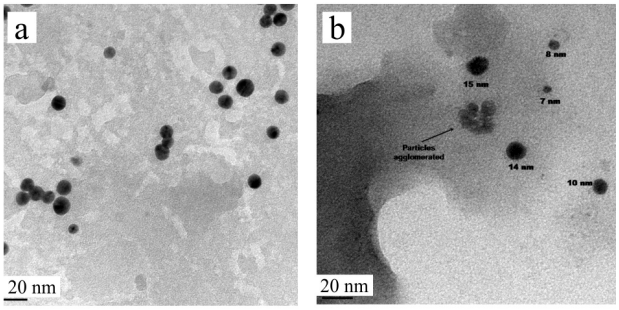

Figure 1. TEM images of (a) gold nanoparticles and (b) silver nanoparticles.

Figure 2 shows the absorption spectra of the nanoparticles in solution and of the assembled multilayer films with 20 and 5 layers of gold and silver nanoparticles, respectively. By increasing the number of layers to the ideal thickness, a 73% increase in absorbance was observed (inset, Figure 2) for both systems. The absorption spectrum of gold nanoparticles in solution presents a maximum resonance mode at ca. 525 nm, characteristic of nanoparticles with ca. 30 nm in diameter[32,33] (Figure 2a). The absorption spectrum of silver nanoparticles in solution presents a maximum resonance mode at ca. 400 nm characteristic of nanoparticles with ca. 5 nm in diameter.[34] Both gold and silver nanoparticle multilayer films display a maximum resonance peak redshift of ca. 70 nm when compared to the respective nanoparticles in solution. Although silver nanoparticles in solution present a narrower resonance mode than gold, the opposite behavior is observed for the multilayer films. These results were expected, once colloidal silver nanoparticles are well known to present sharper

absorption peaks.[34,35] However, when assembled in a film, the nanoparticles seems to be more likely to agglomerate, behaving as larger particles. In addition, two other factors must be taken into account: the strong interaction between nanoparticles in adjacent layers resulting in redshifts of the plasmonic mode due to dipole interactions,[36-39] and the electrochemical reactivity of silver, which oxidizes easily, resulting in a change in surface refractive index and therefore in a redshift of the maximum resonance mode. All these characteristics result in a wider absorption band of silver nanoparticle film when compared to gold. An important conclusion obtained from these results is that the multilayer films keep their plasmonic properties allowing one to apply this system on the development of miniaturized SPR based sensors.

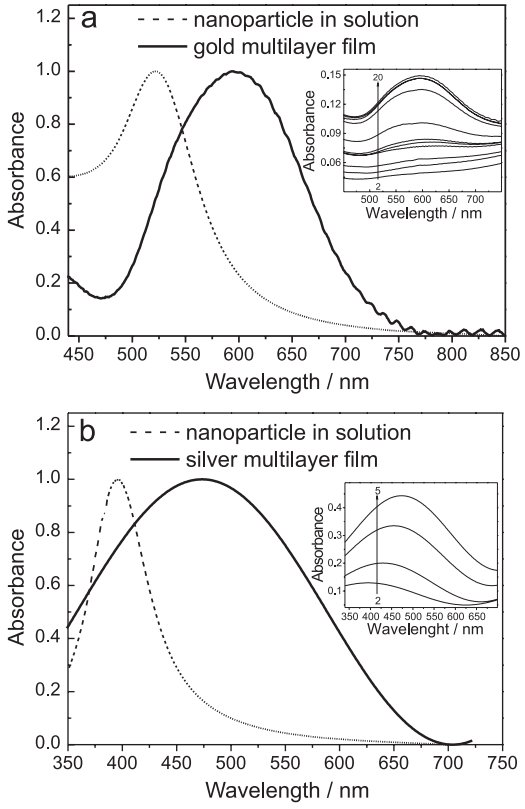

Figure 2. Absorption spectra from (a) gold nanoparticles in solution, gold multilayer film (20 layers), (b) silver nanoparticles in solution and silver multilayer film (5 layers). Insets: Absorbance as a function of the number of layers from (a) gold and (b) silver nanoparticles multilayer films.

The effect of temperature on the plasmon resonance was investigated in the temperatures of 9 °C and 25 °C (not shown). Although the intensity of plasmonic band slightly decreases at higher temperatures, the resonance mode remains the same. Hence, the analytical performance of the plasmonic sensor is not affected by temperature variations within this range. In addition, the decrease in intensity is larger for silver than for gold nanoparticles, and a reasonable hypothesis to explain this result is related to the size of the nanoparticles.[32]

Cyclic voltammetry blocking experiments were applied to evaluate the surface coverage of the substrate after assembling the nanoparticle multilayers (Figure 3). One can observe the characteristic redox process of $K_3[Fe(CN)_6]$ displaying an anodic peak at ca. 0.34 V and a cathodic peak at ca. 0.18 V (vs. Ag/AgCl).[36] In addition, the assembling of gold nanoparticles resulted in a dramatically decrease of current, due to the limited diffusion of $Fe(CN)_6^{3-}$ species toward the FTO. The MPTMS molecules, used as linker, block the charge conduction through the layers of nanoparticles towards the FTO. Therefore as consequence of a high surface coverage, the redox process of $K_3[Fe(CN)_6]$ was almost completely blocked by the gold and silver nanoparticle multilayers films. For electrochemical sensor application, one should work with lower number of nanoparticles layers to avoid decreasing the electrode electroactivity.

The small capacitance effect observed in curves (b) and (c) (Figure 3) is attributed to the stray capacitance formed between the nanoparticles and the electrolytic solution. In addition, both voltammograms on gold and silver multilayer do not present sigmoidal waves as earlier reported in the literature.[40,41]

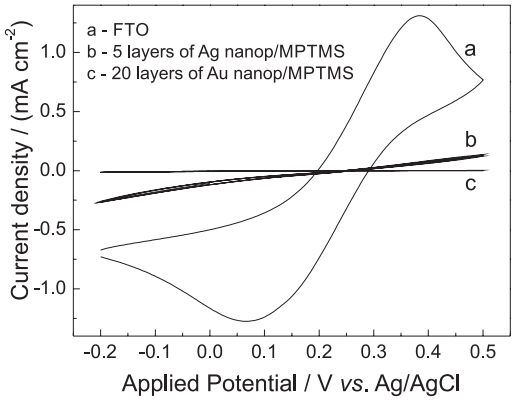

Figure 3. Voltammograms of 1 mmol L^{-1} of $K_3[Fe(CN)_6]$ and 0.1 mol L^{-1} of KCl solution on (a) bare FTO electrode, (b) 5 layers of silver nanoparticles covered FTO electrode and (c) 20 layers of gold nanoparticles covered electrode.

The inset in Figure 4 shows the normalized absorption spectra for the gold nanoparticles based sensor in glucose solution. The sensor response is related to the sensitivity to changes in the refractive index at the nanoparticles local environment.[42] By monitoring changes in the resonance mode at different refractive index (from 1.334 to 1.359), one can observe ca. 6 nm redshift of the maximum resonance and the bulk sensitivity of ca. 220 nm ± 33 nm RIU^{-1}.

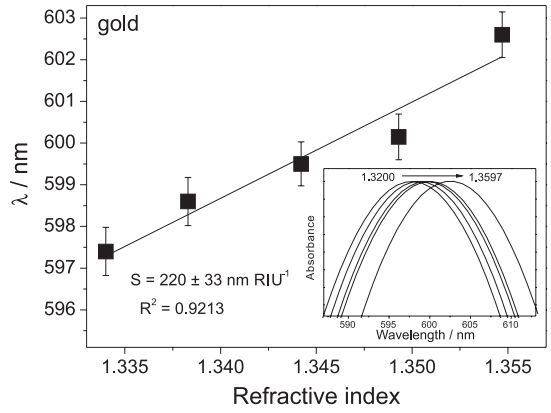

Figure 4. Surface plasmon resonance position of gold nanoparticle multilayer film (20 layers) as a function of the refractive index. Inset: normalized absorption spectra of gold plasmonic substrate in different refractive index.

The inset in Figure 5 shows the normalized absorption spectra of silver nanoparticle based sensor in glucose solution. As observed for the gold nanoparticles film, a redshift of the maximum resonance mode is obtained by increasing the refractive index at the nanoparticles local environment. The redshift was measured as ca. 4 nm for the range of refractive index studied and the sensitivity was calculated as ca. 140 ± 10 nm RIU^{-1}. In addition to sensitivity, the FOM is an important factor to characterize the performance of a sensor, as it takes into account the full width at half maximum (FWHM) of the plasmon resonance mode (FOM = sensitivity / FWHM), allowing a sensor performance to be compared to other systems. The FOM obtained for the gold and silver nanoparticles multilayer films were 7.0 and 0.6 RIU^{-1}, respectively.

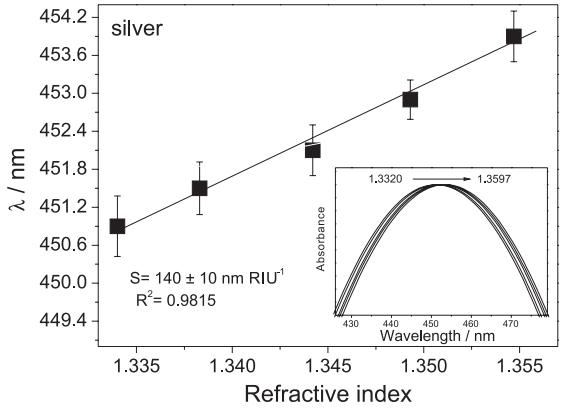

Figure 5. Surface plasmon resonance mode of silver nanoparticle multilayer film (5 layers) as a function of the refractive index. Inset: normalized absorption spectra of silver plasmonic substrate in different refractive index.

Gold multilayer films presented higher sensitivity and FOM than silver films. This result was already expected due to the optical behavior of the films (Figure 2b). In addition, the FOM obtained from the gold nanoparticle multilayer film displays an improvement when compared to literature.[19-23] We suggest that this result was achieved due to our preliminary study to determine the optimum number of layers to assemble a high sensitivity platform, in addition to the well controlled method to synthesize and chemically adsorb the nanoparticles.

Preliminary studies showed non-linearity for the sensitivity as a function of the number of layers. This behavior may be result of the agglomeration process taking place at thicker films, resulting in larger plasmon modes and therefore in lower FOM, as well as lower sensitivity. The films obtained in this work presented high reproducibility for sensing measurements; in addition, by cyclic voltammetry blocking experiments, we have observed the stability of the films for at least three months.

Nanoparticle surface binding measurements were carried out using the biotin-streptavidin system due to their extremely high binding affinity (K_a 10^{13} $(mol\ L^{-1})^{-1}$).[43] This property is one of the main reasons for the application of this scheme in biosensing detectors, since it allows the use of harsh conditions during biochemical assays. Additionally, the specificity of the interaction allows uniformly oriented protein immobilization, providing an important advantage over other immobilization techniques.[44] Streptavidin, a tetrameric protein, can bind up to four biotinylated molecules (i.e., antibodies, inhibitors, nucleic acids, etc.) with minimal impact on its biological activity and therefore, will provide a ready pathway for extending the analyte accessibility of the SPR nanobiosensor. The biotin-streptavidin system has been studied in detail by SPR spectroscopy.[45-47]

The SPR peaks from each step in the assembly of bio-recognition process were measured while flowing a PBS solution over the multilayer film. Figure 6 shows the results of protein binding experiments, related to the gold (Figure 6a) and the silver nanoparticles multilayer films (Figure 6c). The wavelength redshifts ($\Delta\lambda$) were calculated using the SPR absorption band of cysteamine as reference and plotted in Figures 6b and 6d, for gold and silver nanoparticles multilayer films, respectively. The total surface assembly process (cysteamine-biotin linker-streptavidin) corresponded to a resonance band redshifts of ca. 5 nm for both plasmonic sensorial substrates, indicating an increase in the surface-average refractive index, as expected from protein adsorption.[48]

Conclusion

In this work, we presented a very simple method to assemble biosensors with high sensitivity. The

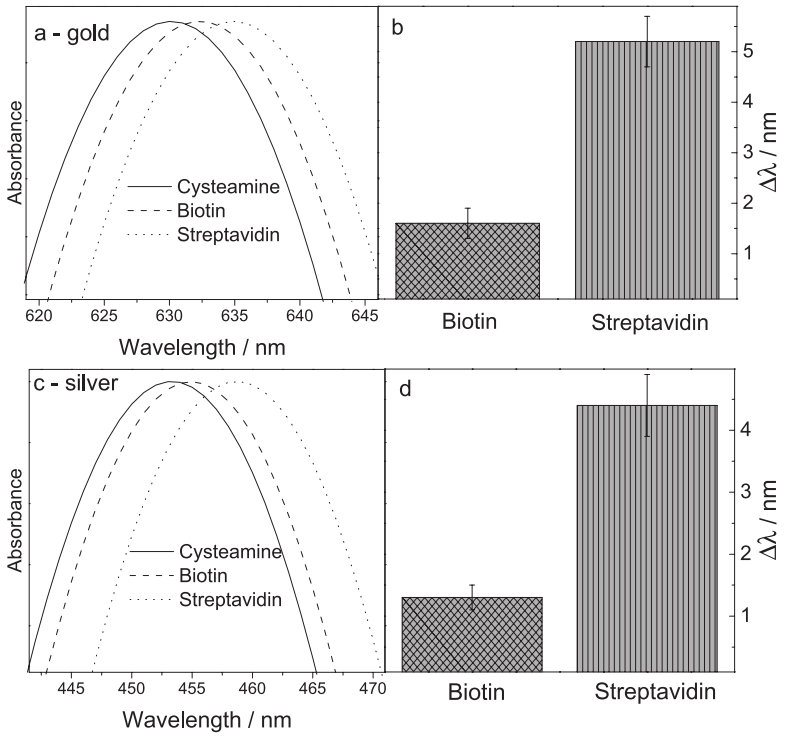

Figure 6. Application of gold nanoparticle multilayer film (on top) and silver nanoparticle multilayer film (bottom) to detect surface binding in the assembly process of cysteamine monolayer-biotin linker-streptavidin protein system. (b) and (d) SPR shift measured relative to cysteamine after the adsorption of biotin and streptavidin on the nanoparticles.

integrated device was successfully applied to detect changes in refractive index, presenting sensitivity and FOM of 220 ± 33 nm RIU^{-1} and 7.0 RIU^{-1} for gold nanoparticles, and 140 ± 10 nm RIU^{-1} and 0.6 RIU^{-1} for silver nanoparticles. The nanoparticles sensitivity was exploited to detect surface binding in the assembly process of cysteamine monolayer-biotin linker-streptavidin protein system. In the protein binding event monitoring experiments, the average shifts in resonance wavelength was ca. 5 nm for both gold and silver multilayer films. The plasmonic substrates developed in this work might be further applied on the detection of different analytes, such as cancer biomarkers and pesticides.

Acknowledgments

We gratefully acknowledge funding support and scholarships for this work from FAPERGS (ARD – no. 11/0497-0), CNPq (Universal no. 477491/2012-0), CNPq/CAPES (Casadinho no. 552197/2011-4), Universidade Federal de Pelotas and Universidade Federal do Rio Grande do Sul.

References

1. Nice, E. C.; Catimel, B.; *BioEssays* **1999**, *21*, 339.
2. Vo-Dinh, T.; Cullum, B.; *J. Anal. Chem.* **2000**, *366*, 540.
3. Nath, N.; Chilkoti, A.; *J. Anal. Chem.* **2002**, *74*, 504.
4. Xiao,Y.; Patolsky, F.; Katz, E.; Hainfeld, J. F.; Willner, I.; *Science* **2003**, *299*, 1877.
5. Schierhorn, M.; Lee, S. J.; Boettcher, S. W.; Stucky, G. D.; Moskovits, M.; *Adv. Mater.* **2006**, *18*, 2829.
6. Cai, H.; Xu, Y.; Zhu, N.; He, P.; Fang,Y.; *Analyst* **2002**, *127*, 803.
7. Eck, D.; Helm, C. A.; *Langmuir* **2001**, *17*, 957.
8. Shankaran, D. R.; Gobi, K. V.; Miura, N.; *Sens. Actuators, B* **2007**, *12*, 158.
9. Wang, J.; Polsky, R.; Xu, D.; *Langmuir* **2001**, *17*, 5739.
10. Wang, J.; Xu, D.; Polsky, R.; *J. Am. Chem. Soc.* **2002**, *124*, 4208.
11. McKenzie, K. J.; Marken, F.; *Langmuir* **2003**, *19*, 4327.
12. Milsom, E. V.; Perrott, H. R.; Peter, L. M.; Marken, F.; *Langmuir* **2005**, *21*, 9482.
13. Amiri, M.; Shahrokhian, S.; Marken, F.; *Electroanal.* **2007**, *19*, 1032.
14. Im, H.; Lee, S. H.; Wittenberg, N. J.; Johnson, T. W.; Lindquist, N. C.; Nagpal, P.; Norris, D. J.; Oh, S.-H.; *ACS Nano* **2011**, *5*, 6244.
15. Lee, S. H.; Bantz, K. C.; Lindquist, N. C.; Oh, S.-H.; Haynes, C. L.; *Langmuir* **2009**, *25*, 13685.
16. Gao, H. W.; Yang, J. C.; Lin, J. Y.; Stuparu, A. D.; Lee, M. H.; Mrksich, M.; Odom, T. W.; *Nano Lett.* **2010**, *10*, 2549.

17. Menezes, J. W.; Ferreira, J.; Santos, M. J. L.; Cescato, L.; Brolo, A. G.; *Adv. Funct. Mater.* **2010**, *20*, 3918.
18. Valsecchi, C.; Brolo, A. G.; *Langmuir* **2013**, *29*, 5638.
19. De Leebeeck, A.; Kumar, L. K. S.; de Lange, V.; Sinton, D.; Gordon, R.; Brolo, A. G.; *Anal. Chem.* **2007**, *79*, 4094.
20. Ferreira, J.; Santos, M. J. L.; Rahman, M. M.; Brolo, A. G.; Gordon, R.; Sinton, D.; Girotto, E. M.; *J. Am. Chem. Soc.* **2009**, *131*, 436.
21. Vazquez-Mena, O.; Sannomiya, T.; Villanueva, L. G.; Voros, J.; Brugger, J.; *ACS Nano* **2011**, *5*, 844.
22. Dong, P.; Lin, Y.; Deng, J.; Di, J.; *Appl. Mater. Interfaces* **2013**, *5*, 2392.
23. Sachan, R.; Yadavali, S.; Shirato, N.; Krishna, H.; Ramos, V.; Duscher, G.; Pennycook, S. J.; Gangopadhyay, A. K.; Garcia, H.; Kalyanaraman, R.; *Nanotechnology* **2012**, *23*, 275604.
24. Eftekhari, F.; Escobedo, C.; Ferreira, J.; Duan, X.; Girotto, E. M.; Brolo, A. G.; Gordon, R.; Sinton, D.; *Anal. Chem.* **2009**, *81*, 4308.
25. Escobedo, C.; Chou, Y.-W.; Rahman, M.; Duan, X.; Gordon, R.; Sinton, D.; Brolo, A. G.; Ferreira, J.; *Analyst* **2013**, *138*, 1450.
26. Monteiro, J. P.; Carneiro, L. B.; Rahman, M. M.; Brolo, A. G.; Santos, M. J. L.; Ferreira, J.; Girotto, E. M.; *Sens. Actuators, B* **2013**, *178*, 366.
27. Monteiro, J. P.; Ferreira, J.; Sabat, R. G.; Rochon, P.; Santos, M. J. L.; Girotto, E. M.; *Sens. Actuators, B* **2012**, *174*, 270.
28. Turkevich, J.; Stevenson, P. C.; Hillier, J.; *Discuss. Faraday Soc.* **1951**, *11*, 55.
29. Zhu, T.; Vasilev, K.; Kreiter, M.; Mittler, S.; Knoll, W.; *Langmuir* **2003**, *19*, 9518.
30. Van Hyning, D. L.; Zukolski, C. F.; *Langmuir* **1998**, *14*, 7034.
31. Fan, M.; Brolo, A. G.; *Phys. Chem. Chem. Phys.* **2009**, *11*, 7381.
32. Link, S.; El-Sayed, M. A.; *J. Phys. Chem. B* **1999**, *103*, 4212.
33. He, Y. Q.; Liu, S. P.; Kong, L.; Liu, Z. F.; *Spectrochim. Acta, Part A* **2005**, *61*, 2861.
34. Badr, Y.; Wahed, M. G. A. E.; Mahmoud, M. A.; *Appl. Surf. Sci.* **2006**, *253*, 2502.
35. Choi, S. H.; Kim, Y. L.; Byun, K. M.; *Opt. Express* **2011**, *19*, 458.
36. Malikova, N.; Pastoriza-Santos, I.; Schierhorn, M.; Kotov, N. A.; Liz-Marzan, L.-M.; *Langmuir* **2002**, *18*, 3694.
37. Mamedov, A. A.; Belov, A.; Giersig, M.; Mamedova, N. N.; Kotov, N. A.; *J. Am. Chem. Soc.* **2001**, *123*, 7738.
38. Ung, T.; Liz-Marzan, L. M.; Mulvaney, P.; *J. Phys. Chem. B* **2001**, *105*, 3441.
39. Caruso, F.; Spasova, M.; Salgueirino-Maceira, V.; Liz-Marzan, L. M.; *Adv. Mater.* **2001**, *13*, 1090.
40. Shen, Y.; Wu, T.; Zhang, Y.; Li, J.; *Talanta* **2005**, *65*, 481.
41. Szunerits, S.; Boukherroub, R.; *Electrochem. Commun.* **2006**, *8*, 439.
42. Englebienne, P.; *Analyst* **1998**, *123*, 1599.
43. Haes, A. J.; Duyne, R. P. V.; *Anal. Bioanal. Chem.* **2004**, *379*, 920.
44. Rusmini, F.; Zhong, Z.; Feijen, J.; *Biomacromolecules* **2007**, *8*, 1775.
45. Jung, L. S.; Campbell, C. T.; *J. Phys. Chem. B* **2000**, *104*, 11168.
46. Perez-Luna, V. H.; O'Brien, M. J.; Opperman, K. A.; Hampton, P. D.; Lopez, G. P.; Klumb, L. A.; Stayton, P. S.; *J. Am. Chem. Soc.* **1999**, *121*, 6469.
47. Green, N. M.; *Adv. Protein Chem.* **1975**, *29*, 85.
48. Jung, L. S.; Nelson, K. E.; Campbell, C. T.; Stayton, P. S.; Yee, S. S.; Perez-Luna, V.; Lopez, G. P.; *Sens. Actuators, B* **1999**, *54*, 137.

Submitted: October 24, 2013
Published online: April 4, 2014